

The Effects of Porous Baffles on the Hydraulic Performance of Sediment Retention Ponds — A Numerical Modelling Study

Mingqi Guo, Danial Goodarzi, Sina Borzooei, Jonathan Pearson, and Soroush Abolfathi

Abstract—This study develops a numerical model for investigating the hydraulic characteristics of a retention pond with porous baffles. The numerical model is developed using the Reynolds-averaged Navier-Stokes equations (RANS) with $k-\epsilon$ turbulence closure model. The model is successfully validated using physical modelling measurements. The proposed model is used to investigate the key mechanisms that govern and influence the hydraulic efficiency of retention ponds with porous baffles. Three configurations with varying numbers and locations of baffles are simulated. The numerical results are analyzed by comparison of velocity fields, tracer transport patterns, and associated residence time distributions (RTDs) across all the simulation scenarios. It was found that the porous baffles effectively improve hydraulic performance by creating uniform flow distribution and dissipating the flow energy, thereby avoiding dead zones and mitigating short-circuiting. Results show that the location of the first baffle plays a critical role in the flow momentum dissipation. Carefully considerations are required to determine the optimal number and positions of baffles in a specific system. The numerical RTDs are in good agreement with the physical modelling data, confirming the positive contribution of porous baffles to the overall hydraulic performance of the pond by extending the average tracer residence time.

Index Terms—Hydraulics, numerical simulation, porous baffle, retention pond.

I. INTRODUCTION

Sediment retention ponds are a low cost and efficient solution for removing pollutants and settling total suspended solids from water and wastewater [1]. Retention ponds can offer sustainable low emission treatment of wastewater, and can be used as a secondary treatment after wastewater treatment plants, to further enhance the water quality discharge to the environment [2], [3]. Plug flow condition is typically used to characterize the flow system in retention ponds, assuming that influent flows through the pond at the same velocity without mixing and dispersion in the transport

Manuscript received March 24, 2022; revised June 29, 2022. This work was supported in part by the Natural Environmental Research Council (grant NE/R003645/1), and the China Scholarship Council.

Mingqi Guo, Jonathan Pearson, and Soroush Abolfathi are with the School of Engineering, University of Warwick, Coventry CV4 7AL, UK (e-mail: Mingqi.Guo@warwick.ac.uk, J.M.Pearson@warwick.ac.uk, Soroush.Abolfathi@warwick.ac.uk).

Danial Goodarzi is with the Department of Civil Engineering, University of Ottawa, Ottawa ON K1N 6N5, Canada (e-mail: dani.goodarzi@gmail.com).

Sina Borzooei is with the Department of Data Analysis and Mathematical Modelling, Ghent University, Ghent 9000, Belgium (e-mail: Sina.borzooei@ugent.be).

direction [4], [5]. However, the practical hydraulic and hydrodynamic conditions in a constructed retention pond always deviate from the ideal conditions, characterized by the underlying physical transport mechanisms, including short-circuiting and mixing. These processes are capable of severely impairing the effectiveness of ponds for pollutant retention through reducing the effective volume, and thus, reducing the average pollutant residence time [6]. In general, mixing in retention ponds is induced by turbulent diffusion and wind stress, which can affect the pond hydraulics performance by altering the vertical and transverse velocity structures across the pond [4]. Short-circuiting occurs as a result of preferential high-velocity pathways generation that facilitates fluid parcels (e.g. pollutants) to be rapidly transported through the system without an appropriate level of treatment [7]. The short-circuiting events can be exacerbated by extreme climatic events that can significantly change the input flow characteristic and the hydrodynamic structure across the pond [8].

One of the solutions to improve the treatment performance of retention ponds is hydraulic enhancement and geometrical reconfigurations, including inlet and outlet structure, pond geometrical shape, surface berm, island, slope of the sidewalls, and baffles. Installation of retrofitting structures such as baffles can effectively improve the hydraulic performance and reduce the operational costs of retention ponds [9]. Compared to the solid baffles widely used for pond hydraulics optimization [10], permeable baffles with adjustable porosity exhibit better behaviour in pollutant treatment due to their superior capacity of influent distribution, incoming flow energy dissipation, and turbulent momentum damping [11]. Thaxton, Calantoni, and McLaughlin [11] argued that different baffle permeability corresponds to different functional regimes, and determining an optimal baffle permeability under specific conditions is necessary to achieve the most effective hydraulic performance and operational control. Although previous studies have provided practical guidance for porous baffle selection and installation, it is still challenging to obtain a consistent consensus on the best baffle configuration to improve the treatment capacity of retention ponds [12]. Moreover, there remains a limited understanding of the hydraulic characteristics of retention ponds featured by porous baffles.

The hydraulic performance of wastewater stabilization ponds is widely assessed in terms of the characteristics of residence time distribution curves (RTDs) generated from tracer studies [13], which are considerably affected by the combined effects of mixing and short-circuiting processes

[14]. Various hydraulic indices are also derived from RTDs to quantify the primary hydrodynamic processes and assess the overall performance of the hydraulic system. However, the analysis based on RTDs is solely dependent on monitoring the tracer concentration variations at the inlet and outlet, completely ignoring the specific hydraulic processes occurring within the system. Thus, RTD analysis methodology can be identified as a black-box approach [15], which can provide limited information on the mechanisms governing the hydraulic performance of retention ponds. With advances in computational power and numerical simulation algorithms, CFD models have become a powerful tool with the capacity of numerically simulating complex fluid dynamic and pollution transport problems with spatiotemporally varying hydrodynamic behaviour [16]. CFD tools can be adopted to address the current information gaps in understanding pollution transport processes in retention ponds, undertaking detailed RTDs analysis, and enable robust evaluations of the hydraulic efficiency of natural capital water and wastewater treatment ponds [6]. However, CFD models involve many inherent assumptions, and accordingly, they need to be fully verified against the physical modelling experiments or highly resolved numerical simulation data [17].

This study develops a numerical model to investigate the effect of porous baffles on the hydraulic performance of a retention pond. The numerical model developed in this study is validated against the physical modelling measurements previously conducted by Farjood, Melville, and Shamseldin [18]. Three numerical simulation scenarios are developed and simulated with the proposed numerical model to compute the hydraulic performance indicators and tracer transport processes in retention ponds with different numbers and locations of porous baffles. The variations in the velocity fields, streamline patterns, and turbulent kinetic energy distributions are compared across the simulation scenarios to assess the performance of the porous baffles, and illustrate the hydraulic mechanisms controlling the system response to alterations of the baffles. Subsequently, the distributions of passive tracer concentration and RTDs are determined to further reveal the complex relationship between porous baffle retrofitting and the pond hydraulic efficiency.

II. RESEARCH METHODOLOGY

A. Numerical Modelling Approach

The numerical model is developed in an open-source numerical platform, OpenFOAM, designed for numerically solving continuum mechanic problems based on a tensorial approach and three-dimensional finite-volume method (FVM). Reynolds-averaged Navier-Stokes (RANS) equations are used as the governing equations for fluid motion [19]. The continuity equation and momentum equation for incompressible fluid is adopted as:

$$\frac{\partial U_i}{\partial x_i} = 0 \quad (1)$$

$$\frac{\partial U_i}{\partial t} + U_j \frac{\partial U_i}{\partial x_j} = -\frac{1}{\rho} \frac{\partial p}{\partial x_i} + \frac{\partial}{\partial x_i} \left(\nu \frac{\partial U_i}{\partial x_i} - \overline{u_i u_j} \right) + S_i \quad (2)$$

where U_i is time-averaged velocity component in i direction, $i = x, y, z$; p is time-averaged pressure; t is time; ρ is fluid density; ν is kinematic viscosity; x_i and x_j are the spatial location vectors in $x, y,$ and z axis direction, respectively.

The turbulence treatment is the key aspect of CFD models, and this study adopts the standard $k - \varepsilon$ turbulence closure model to approximate the Reynolds stresses ($\overline{u_i u_j}$) of turbulent flows [20], depicted as:

$$\overline{u_i u_j} = \nu_t \left(\frac{\partial U_j}{\partial x_i} + \frac{\partial U_i}{\partial x_j} \right) + \frac{2}{3} k \delta_{ij} \quad (3)$$

$$\nu_t = c_\mu \frac{k}{\varepsilon} \quad (4)$$

where δ_{ij} is Kronecker delta, k is turbulence kinetic energy, ε is the turbulence kinetic energy dissipation rate, and ν_t is the turbulent viscosity.

The Darcy-Forchheimer relation is applied to characterize the flow through baffles by using (5), representing the viscous and inertial resistance in the porous regions [21]:

$$S_i = -(\nu D + \frac{1}{2} |J| F) \overline{u_i} \quad (5)$$

The coefficients D and F are calculated based on the baffle porosity ($\varepsilon, 61\%$) and median diameter ($d_{50}, 3.300$ mm) [21]:

$$D = \frac{150}{d_{50}^2} \frac{(1-\varepsilon)^2}{\varepsilon^3} \quad (6)$$

$$F = \frac{1.75(1-\varepsilon)}{d_{50}^2 \varepsilon^3} \quad (7)$$

Once the hydrodynamic simulation obtains a stable hydraulic condition, the unsteady transport of a conservative tracer quantities C will be simulated by solving the advection-diffusion equation:

$$\frac{\partial C}{\partial t} + U_j \frac{\partial C}{\partial x_j} = D_t \frac{\partial^2 C}{\partial x_j^2} \quad (8)$$

where D_t is the turbulent diffusivity.

B. Simulation and Boundary Condition Setup

In OpenFOAM, the governing equations are solved by finite-volume discretization methods using structured grids. Thus, the simulated ponds with dimensions of 3.1 m (height) \times 1.49 m (Width) \times 0.27 m (Depth) and 2:1 (Horizontal: Vertical) bank slope are constructed in the simulations by applying *blockMesh* and *snappyHexMesh* (Fig. 1). The inlet surface is located on the upper edge of the pond and perpendicular to the front wall. The outlet structure is simplified to several 2 mm-thickness rings attached to the cylinders with 48 mm diameter, and the cylinders are further fixed to the outlet riser at 220 mm height. Porous baffles are placed in three positions perpendicular to the inflow path,

with a height of 270 mm, and across the full pond width with 10 mm thickness. The numerical models developed for the three simulation scenarios shown in Fig. 1, with a total of 1496575 (C123), 1448310 (C23), and 1446444 (C13) cells, respectively.

Table I summarises the boundary conditions used for the numerical model development. At the inlet patch, a Dirichlet boundary condition is applied for the velocity and turbulence variables according to the constant flow rate used in physical experiments (e.g. 2 L/s).

The standard solver simpleFoam is adopted by this study for steady-state simulations. In the numerical solution, Gaussian with linear interpolation is selected for both numerical gradient schemes and Laplacian schemes, and an explicit non-orthogonal correction is additionally employed to the later schemes. For divergent schemes, the first-order accurate upwind schemes and the second-order accurate linear schemes are used, respectively, to discretize the convective and diffusive terms of vectors in the governing equations to reduce the truncation errors in the discretization process of partial differential equations [21]. A first-order Euler method is adopted for the discretization of time derivatives in the governing equations. A semi-implicit method for pressure-linked equations (SIMPLE) algorithm is adopted to generate the final solution by consecutively developing pressure and velocity fields following the momentum and continuity equations at every iteration [22]. In the tracer study, the initial time step starts from 500 s, at which time the system has generated a steady-state velocity field, and the time step is set to 0.05 s, assuring the stability of the explicit time discretization scheme. The tracer with a constant concentration is injected into the computational domain from the pond surface, and the complete transport simulation runs for 2500 s to make sure all tracers leave the pond completely. The tracer concentration at the outlet is normalized by the total amount of injected tracer and used to generate corresponding RTDs for model validation.

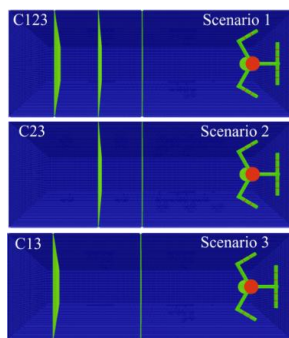


Fig. 1. Three-dimensional view of the meshed computational domain for the three scenarios.

TABLE I: BOUNDARY CONDITIONS OF THE NUMERICAL MODEL

Boundary Condition	U	P	k	ϵ
Surface	slip	zero-Gradient	kqRWall-Function	epsilonWall-Function
InletWater	flowRate-InletVelocity	zero-Gradient	fixed-Value	fixed-Value
Outlet	inletOutlet	fixed-Value	zero-Gradient	zero-Gradient
Bottom	noSlip	zero-Gradient	kqRWall-Function	epsilonWall-Function

C. Hydraulic Performance

To assess the hydraulic performance of individual pond under the combined effects of short-circuiting and mixing in the proposed systems, the residence time distribution (RTD) of individual tracer study is computed by normalizing the outlet tracer concentration versus time, $E(t)$, written as [18]:

$$E(t) = \frac{c / c_0}{\int_0^{\infty} c(t) dt} \quad (9)$$

$$\tau = \frac{t}{t_n} \quad (10)$$

where c / c_0 and τ is the normalized concentration and time, respectively, c_0 presents the total mass of the injected tracer versus the pond volume, and t_n denotes the nominal hydraulic residence time (HRT).

III. RESULTS AND DISCUSSION

A. Flow Characteristics

Fig. 2 (a), (e), and (i) depict the streamline patterns for the three simulation scenarios (see Fig. 1) with varying baffle-retrofitting. The analysis of the results shows that flow features in all ponds are substantially characterized by the baffle layouts. It is demonstrated that the installation of porous baffles can effectively distribute the flow and generate uniform flow streamlines, conducive to maintaining the effective volume for near-plug flow conditions. Typically, streamlines in the three-baffle pond (C123 scenario) gradually evolve into two-dimensional flow structures from inlet to outlet and exhibit a uniform distribution across the pond width. Similar flow structures are also developed in two-baffle ponds (C13 and C12 scenarios). However, streamlines affected by the chamber width tend to be concentrated near the pond wall, forming low-velocity regions in the middle of these two systems. Such discrepancy proves that increasing the baffle number can lead to a more even distribution of flow pathways across the pond, while an inappropriate number and location for the porous baffle retrofitting may reduce the hydraulic performance of the system. Hence, it is important to determine the optimal number and location for baffles.

The results highlight the formation of a recirculation zone in the first chamber for all the simulation cases. Given that the inflow rate remains consistent for all the simulated scenarios, the recirculation zone is generated due to the pond configuration. In hydraulic retrofits, the first baffle is commonly considered to play the most crucial role as it can dissipate most of the inflow energy [18]. Flow patterns in C123 and C13 illustrate that the earlier the influent momentum dissipates by the first baffle (Fig. 2 (d), (h), and (l)), the sooner the system reaches a steady state, and thus the effective volume of the pond grows. Conversely, increasing the distance of the baffle from the inlet, as suggested by C23, leads to longer flow paths with higher velocity (Fig. 2 (f)) and the formation of large recirculation structures with high kinetic energy viscosity (Fig. 2 (h)). Therefore, the tracer

mixing process will be enhanced in the water column in case C23, along with the reduction of effective volume.

As depicted by Fig. 2 (b), (f), and (j), a clear short-circuiting mechanism can be observed on the water surface, which is the most significant in the first chamber. In fact, the short-circuiting phenomenon can be associated with porous baffles. Although the baffles introduced in the simulations allow water to pass through their porous medium with more uniform distributions and lower velocity values, the development of recirculation caused by momentum dissipation inevitably reduces the effective volume of the first chamber, leading to the generation of preferred faster flow paths on the water surface. Therefore, significant velocity variations can be found in the first compartment. Furthermore, since near-wall fluid usually has minimal mixing with the adjacent fluid, the surface short-circuiting effect is also formed along the pond sidewalls.

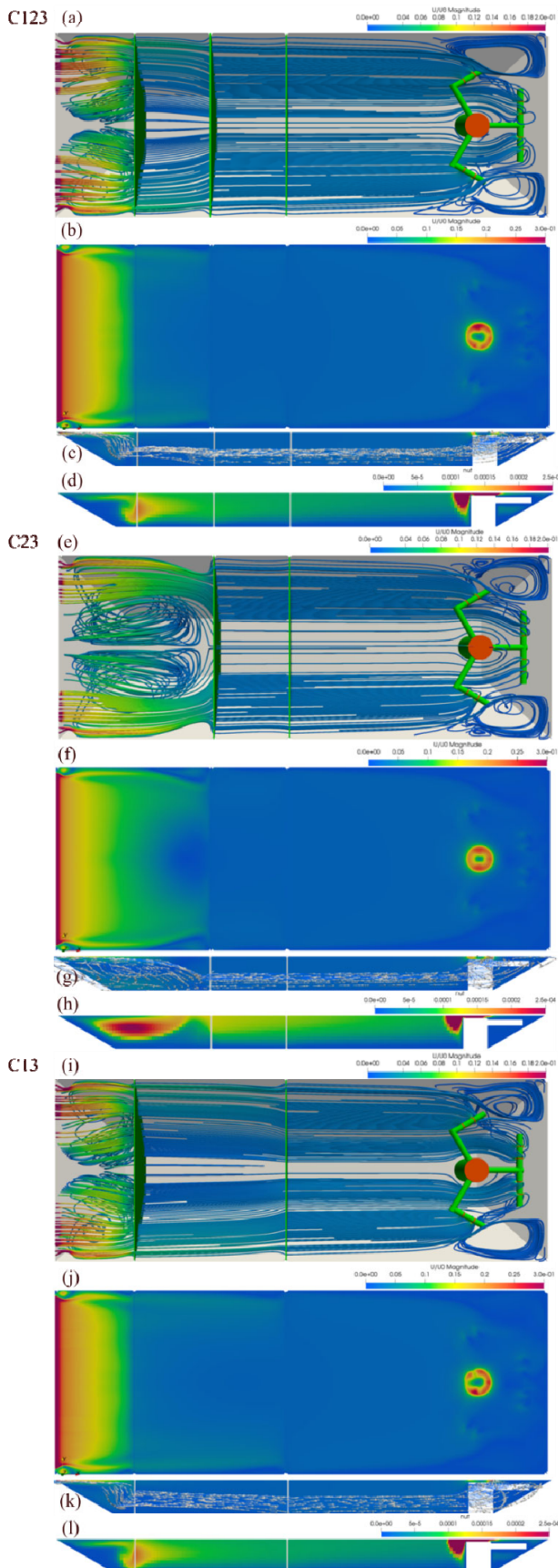
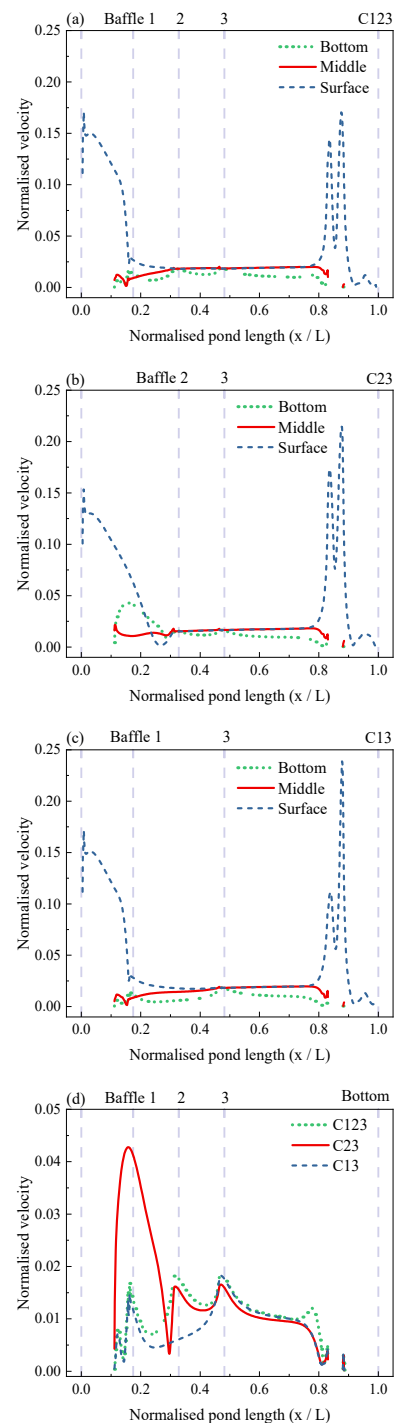


Fig. 2. Hydraulic characteristics of the retention ponds with different baffle configurations: (a), (e), and (i) present streamlines on the $x - y$ plane; (b), (f), and (j) illustrate the free surface velocity on the $x - y$ plane; (c), (g), and (k) show the velocity on the $x - z$ plane at the midspan; (d), (h), and (l) depict the turbulent kinematic viscosity ν_t on the $x - z$ plane at the midspan.



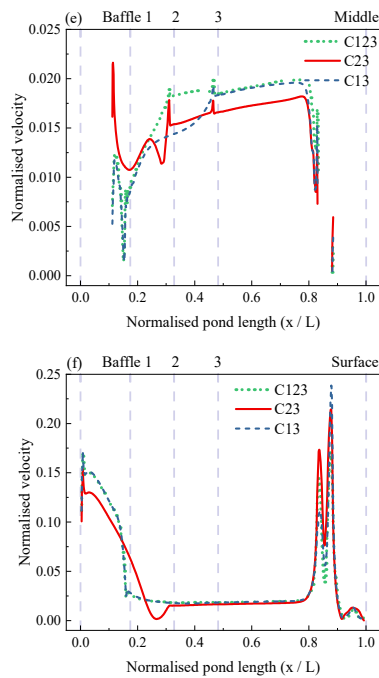


Fig. 3. Time-averaged velocity along the longitudinal direction of the pond at the bottom (0.09 m), middle (0.18 m) and surface (0.27 m) of the water column.

In Fig. 3, the horizontal velocity profiles across the pond length are plotted for flow in different depths (e.g. bottom, middle, and surface). The analysis of simulation results highlights the characteristics of velocity structures across the water column, as the surface and middle velocities are normally higher than those values computed for the bottom. The large velocity fluctuations in front of the first baffle are consistent with the observed enhanced surface short-circuiting effect and recirculation regions. The small differences in the velocity profiles at different depths indicate the formation of uniform flow conditions along the water column, which can be attributed to the excellent flow distribution capability of the porous baffle. Fig. 3 (d), (e), and (f) compare the velocity profiles at the same depth between the three simulation scenarios. It is evident that for different porous baffle configurations, similar velocity profiles and fluctuations occurs with overlapping profile shapes appearing at the locations where similar pond configurations exist. This show that the porous baffles can regulate the flow path and velocity and improve the treatment capability of retention ponds.

B. Tracer Study

Fig. 4 shows the instantaneous snapshots of tracer concentration across different time points. At time $t = 100$ s, tracer clouds concentrate on the water surface towards the third baffle in C123 and C13, while a portion of the tracer in C23 is still trapped within the large recirculation zones in the water column of the first chamber. Then, this distinction disappears over time, and tracer tends to demonstrate a similar distribution for all three simulation scenarios, where their concentrations are commonly diffused by the flowing water in the longitudinal direction and generate diluted vertical profiles in the water column. Short-circuiting effects are evident in the snapshots at times $t = 200$ s and $t = 300$ s, as the tracer on the water surface moves faster and reaches the

exit earlier compared to the tracer at the bottom, which still diffuses along the flow direction at the same time point. This is exactly consistent with the velocity structures analyzed in Fig. 3 and ultimately exerts a long-tail effect on the associated RTDs in Fig. 5.

Fig. 5 presents the outlet tracer predictions generated computationally, used to reveal the effect of baffle retrofitting on the hydraulic effectiveness according to the shape and position of the RTDs. At first sight, the normalized concentrations of all RTDs increase rapidly ($\tau < 0.5$) at a high growth rate (close to 1) and display a long tail after reaching the peaks, both of which are consistent with physical experimental measurements [18]. The shape of the RTDs in Fig. 5 are primarily influenced by the short-circuiting effects on the pond water surface, the generation of recirculation zones near the inlet and the slow tracer movement at the pond bottom. However, the number of baffles and their locations did not induce any noticeable discrepancy in the RTDs, in line with the physical modelling results [18]. The RTDs for cases C123 and C13 show a more pronounced second peak compared to case C23, in accordance with the longer transport time of the tracer below the pond in Fig. 4. By contrast, the larger recirculation pattern in C23 allows the tracer in the water column to undergo a better mixing process, therefore reducing the temporal difference in the upper and lower tracer transmission. This result emphasizes the significance of the baffle location on the hydraulic efficiency of the retention pond by affecting the hydrodynamic characteristics.

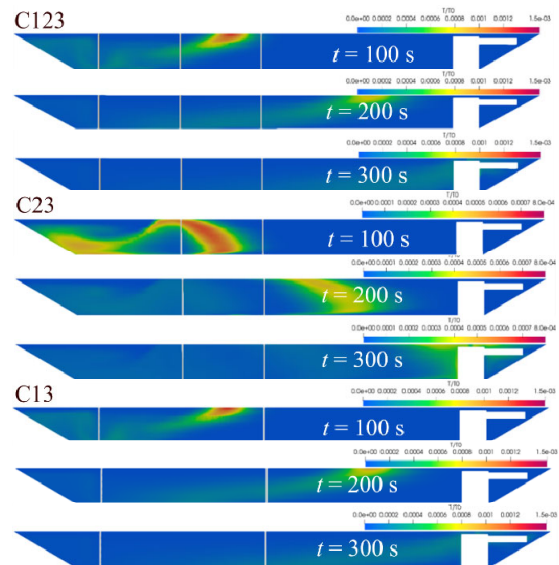
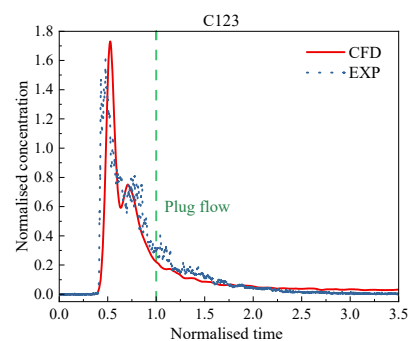


Fig. 4. Tracer concentration snapshots at $t = 100, 200, 300$ seconds after tracer injection in the retention pond; concentration is shown on the $x - z$ plane at midspan ($y = \text{Width} / 2$).



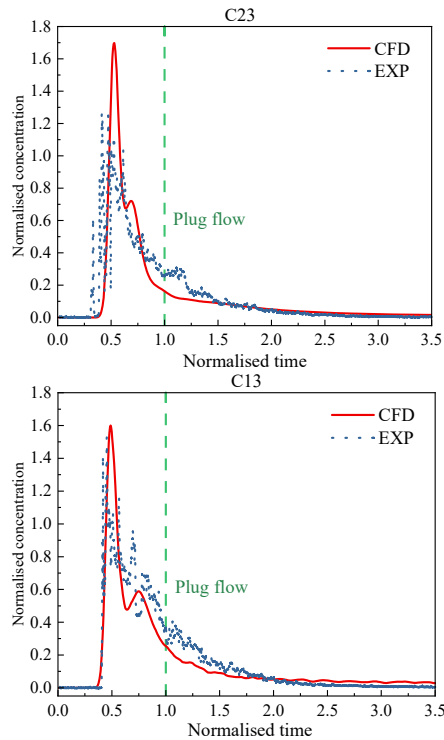


Fig. 5. Normalized RTDs of the pond configurations simulated in this study compared to the physical modelling measurements.

IV. CONCLUSION

This paper develops a Eulerian type grid-based numerical model using RANS governing equations with the standard $k-\epsilon$ turbulence closure model to investigate the performance of retention ponds with porous baffles. The numerical model is validated against the physical modelling measurements [18]. Three simulation scenarios were investigated with varying numbers and locations of porous baffles across the pond. The numerical results were analyzed to investigate flow hydrodynamics and passive tracer transport across the pond. It was shown that porous baffles separate the flow into several chambers, and the flow characteristics within each chamber are mainly affected by recirculation and short-circuit effects. Analysis of the flow patterns across different simulation scenarios demonstrates the significant contributions of the porous baffles in improving the hydraulic performance of the system, primarily through uniforming the flow distribution and dissipating the incoming flow momentum. In particular, it was found that the first baffle plays a vital role in improving the hydraulic conditions, as its position considerably influence the development of recirculation zones and the influent turbulent kinetic energy dissipation. Accordingly, different tracer distributions are developed in the simulated cases as the baffle position is varied. Furthermore, the complex relationship between hydraulic efficiency and baffle performance was investigated in this study. Increasing the number of baffles was shown to generate more uniform flow distributions in the water column, and provide a larger effective volume for water treatment. The numerical model proposed in this study can be used to better understand the treatment performance of retention ponds and improve their design and operational conditions.

CONFLICT OF INTEREST

The authors declare no conflict of interest.

AUTHOR CONTRIBUTIONS

Mingqi Guo conducted the research and wrote the paper; Danial Goodarzi revised the paper; Soroush Abolfathi revised the paper; all authors had approved the final version.

ACKNOWLEDGMENT

Mingqi Guo thanks Dr Arash Farjood for providing the physical modelling data.

REFERENCES

- [1] C. S. Thaxton, J. Calantoni, and R. A. McLaughlin, "Hydrodynamic assessment of various types of baffles in a sediment retention pond," *ASAE Trans*, vol. 47, no. 3, pp. 741–750, 2004.
- [2] S. Borzooei, G. H. B. Miranda, S. Abolfathi, G. Scibilia, L. Meucci, and M. C. Zanetti, "Application of unsupervised learning and process simulation for energy optimization of a WWTP under various weather conditions," *Water Sci. Technol.*, vol. 81, no. 8, pp. 1541–1551, Apr 2020.
- [3] S. Borzooei *et al.*, "Energy optimization of a wastewater treatment plant based on energy audit data: Small investment with high return," *Environ. Sci. Pollut. Res.*, vol. 27, no. 15, pp. 17972–17985, May 2020.
- [4] T. R. Headley and R. H. Kadlec, "Conducting hydraulic tracer studies of constructed wetlands: A practical guide," *Ecohydrol. Hydrobiol.*, vol. 7, no. 3–4, pp. 269–282, Jan 2007.
- [5] M. Jimoh and S. Abolfathi, "Modelling pollution transport dynamics and mixing in square manhole overflows," *J. Water Process Eng.*, vol. 45, no. August 2021, p. 102491, Feb 2022.
- [6] M. Ahadi, D. J. Bergstrom, and K. A. Mazurek, "Computational fluid-dynamics modeling of the flow and sediment transport in stormwater retention ponds: A review," *J. Environ. Eng.*, vol. 146, no. 9, p. 03120008, Sep 2020.
- [7] P. R. Schroeder, "Residence time distributions of shallow basins," *J. Environ. Eng.*, vol. 113, no. 6, pp. 1319–1332, Dec 1988.
- [8] S. Borzooei, R. Teegavarapu, S. Abolfathi, Y. Amerlinck, I. Nopens, and M. C. Zanetti, "Data mining application in assessment of weather-based influent scenarios for a WWTP: Getting the most out of plant historical data," *Water. Air. Soil Pollut.*, vol. 230, no. 1, Jan 2019.
- [9] C.-N. Chen, "Design of sediment retention basins," in *Proc. the National Symposium on Urban Hydrology and Sediment Control*, 1975.
- [10] A. Shilton and J. H. Harrison, "Guidelines for the hydraulic design of waste stabilization ponds," Institute of Technology and Engineering, Massey University, 2003.
- [11] C. S. Thaxton, J. Calantoni, and R. A. McLaughlin, "Hydrodynamic assessment of various types of baffles in a sediment retention pond," *ASAE Trans*, vol. 47, no. 3, pp. 741–749, 2004.
- [12] L. X. Coggins, J. Sounness, L. Zheng, M. Ghisalberti, and A. Ghadouani, "Impact of hydrodynamic reconfiguration with baffles on treatment performance in waste stabilization ponds: A full-scale experiment," *Water (Switzerland)*, vol. 10, no. 2, pp. 1–18, Feb 2018.
- [13] A. Farjood, B. W. Melville, A. Y. Shamseldin, K. N. Adams, and S. Khan, "Evaluation of hydraulic performance indices for retention ponds," *Water Sci. Technol.*, vol. 72, no. 1, pp. 10–21, July 2015.
- [14] M. D. Wahl, L. C. Brown, A. O. Soboyejo, J. Martin, and B. Dong, "Quantifying the hydraulic performance of treatment wetlands using the moment index," *Ecol. Eng.*, vol. 36, no. 12, pp. 1691–1699, Dec 2010.
- [15] E. Demirel and M. M. Aral, "Unified analysis of multi-chamber contact tanks and mixing efficiency evaluation based on vorticity field. Part II: Transport analysis," *Water (Switzerland)*, vol. 8, no. 11, 2016.
- [16] S. Abolfathi and J. Pearson, "Application of smoothed particle hydrodynamics (SPH) in nearshore mixing: A comparison to laboratory data," *Coast. Eng.*, vol. 1, no. 35, p. 16, 2017.
- [17] A. Shilton, "Potential application of computational fluid dynamics to pond design," *Water Sci. Technol.*, vol. 42, no. 10–11, pp. 327–334, Nov 2000.
- [18] A. Farjood, B. W. Melville, and A. Y. Shamseldin, "The effect of different baffles on hydraulic performance of a sediment retention pond," *Ecol. Eng.*, vol. 81, pp. 228–232, Aug 2015.

- [19] D. Goodarzi, K. Sookhak Lari, E. Khavasi, and S. Abolfathi, "Large eddy simulation of turbidity currents in a narrow channel with different obstacle configurations," *Sci. Rep.*, vol. 10, no. 1, pp. 1–17, Jul 2020.
- [20] H. Wang and R. A. Falconer, "Simulating disinfection processes in chlorine contact tanks using various turbulence models and high-order accurate difference schemes," *Water Res.*, vol. 32, no. 5, pp. 1529–1543, Mar 1998.
- [21] M. A. Kizilaslan, E. Demirel, and M. M. Aral, "Effect of porous baffles on the energy performance of contact tanks in water treatment," *Water (Switzerland)*, vol. 10, no. 8, pp. 1–15, Aug 2018.
- [22] D. Goodarzi, S. Abolfathi, and S. Borzooei, "Modelling solute transport in water disinfection systems: Effects of temperature gradient on the hydraulic and disinfection efficiency of serpentine chlorine contact tanks," *J. Water Process Eng.*, vol. 37, no. June, p. 101411, Oct 2020.

Copyright © 2022 by the authors. This is an open access article distributed under the Creative Commons Attribution License which permits unrestricted use, distribution, and reproduction in any medium, provided the original work is properly cited ([CC BY 4.0](https://creativecommons.org/licenses/by/4.0/)).



Mingqi Guo is a PhD student in the School of Engineering, University of Warwick. She completed her bachelor's degree in environmental engineering and master's degree in civil engineering from Harbin Institute of Technology. Her research interest is the fate and transport of solutes and solids in freshwater systems.



Danial Goodarzi is a PhD student in the Department of Civil Engineering, University of Ottawa. He obtained his master's degree in civil environmental engineering from Shahid Beheshti University. His research interests focus on computational fluid dynamics, and dynamic transportation of pollutants in the fluid flow.



Sina Borzooei is working at the Department of Data Analysis and Mathematical Modelling and the Centre for Advanced Process Technology for Urban Resource recovery (CAPTURE), Ghent University. His research interests include process optimization of biological systems, water and wastewater treatment, numerical modelling, data analysis, and digital twins.



Jonathan Pearson is an associate-professor in the School of Engineering at the University of Warwick and the head of Warwick Water. He has over 20 years of research experience in coastal and environmental hydraulics, having previously worked at the Universities of Edinburgh and Sheffield. His research interests concentrate on resilient infrastructure from natural hazards and environmental fate of organic pollutants.



Soroush Abolfathi is an assistant professor in water and environmental engineering at the School of Engineering, Warwick University and a member of Warwick Centre for Predictive Modelling. He is currently chair of the Institution of Civil Engineers (ICE) for Coventry and Warwickshire branch and serves as a member (Vice-Chair) of the UK Leadership Team for International Association of Hydro-Environment Engineering and Research (IAHR). His research interests are pollution transport in the environment (solute and microplastics), and resilient infrastructures to natural hazards, climate change and flooding.